Journal of Building Engineering 82 (2024) 108367

Contents lists available at ScienceDirect

Journal of Building Engineering

journal homepage: www.elsevier.com/locate/jobe

Electric arc furnace slag in substitution of quartz for surface treatment of concrete paving slabs

Amaia Santamaría [a,*], Vanesa Ortega-López [b], Marta Skaf [c], Victor Revilla-Cuesta [b], J.M. Manso [b]

[a] Department of Mechanical Engineering, University of Basque Country, UPV/EHU, Escuela de Ingeniería de Bilbao, Plaza Ingeniero Torres Quevedo 1, 48013, Bilbao, Spain
[b] Department of Civil Engineering, University of Burgos, Escuela Politécnica Superior, Calle Villadiego s/n, 09001, Burgos, Spain
[c] Department of Construction, University of Burgos, Escuela Politécnica Superior, Calle Villadiego s/n, 09001, Burgos, Spain

ARTICLE INFO

Keywords:
EAF slag
Dry shake hardener material
Sustainable concrete
Coating concrete paving slab
DSH concrete durability

ABSTRACT

Electric Arc Furnace (EAF) slag, a by-product of the steelmaking industry, also serves as a high-quality aggregate material for structural concrete production. In this research, its use is proposed as a Dry-Shake Hardener (DSH), in substitution of quartz, in concrete paving top coatings. Three concrete paving slab kinds were produced using EAF: one without fibers, another with metallic fibers; and the third with synthetic fibers. Half of each slab was coated with a classical cement-quartz mix and the other half with a novel cement-slag mix. After four years of outdoor aging at the city of Burgos, Spain, the slabs were visually inspected and no significant differences were found between the two coated materials. Impact, skid, and abrasion resistance tests were carried out and showed similar results for both types of coating courses. The result of both the short and long-term water absorption test results indicated, firstly, no short-term water absorption in both cases and, secondly, lower long-term water absorption in the quartz-cement mix. Finally, observation of the oil stain resistance tests on the top coatings led to the conclusion that the cleaning ability is very good. Analyzing all the results, it may be concluded that a new application for EAF slag have been found, it is a suitable material for use as a DSH for coating concrete paving slabs.

1. Introduction

Electric Arc Furnace (EAF) slag, also known as black slag, is a stony, hard, and slightly porous material produced during the acid refining of steel after melting scrap iron in an electric furnace [1]. For some decades, this material has been classified as waste for disposal at dumping sites. Over the past 25 years, however, many researchers have been analyzing this material with a view to its reuse [2–6]. Its properties have transformed it into a competitive by-product for different purposes within the construction sector, especially as aggregate in bituminous [7,8], and hydraulic binder-based mixes [9–13].

Such promising results have inevitably led to the use of this material in some real construction works. For example, it has been used in the foundations of the Kubik demonstration building at the Tecnalia Research Centre, Bilbao [14], the construction of a sea wall and wave breakers at the port of Bilbao [15], and the construction of Bilbao provisional bus station, in the Basque country, Spain.

The members of this research group were encouraged to look for new applications for EAF slag in hydraulic mixes, one of which is

* Corresponding author.
E-mail address: amaia.santamaria@ehu.eus (A. Santamaría).

https://doi.org/10.1016/j.jobe.2023.108367
Received 16 October 2023; Received in revised form 1 December 2023; Accepted 19 December 2023
Available online 20 December 2023

presented in this paper: a Dry-Shake Hardener (DSH) for concrete paving.

When hydraulic concrete pavements are used in heavily frequented pedestrian areas and/or exposed to heavy weights and impacts, it is indispensable to use surface treatments to preserve the integrity, the appearance, and the durability of the concretes; the technology is typically used inside industrial buildings, warehouses, and garages [16], although its outdoor use is also approachable, despite the economic cost.

There are two types of surface treatments that can be used [17]; either a DSH or liquid surface hardener admixtures. Many studies on liquid surface treatment admixtures [18–22] may be found in the literature. Others on the use of DSH applications [17,23–25] can be divided into two groups: metallic-based and non-metallic based hardeners. Nowadays the most common type of non-metallic DSH is a mixture of 60 % quartz or corundum and 40 % dry Portland cement.

The application of DSH improves superficial abrasion, impact strength of slab surface, skid coefficient, and resistance to both chemical attack and water penetration with respect to the properties of the original concrete surface. In cement-based materials, impact resistance mainly depends on the internal friction at the material interface when two materials are not elastically bonded [26].

M. Sadegzadeh et al. [27] observed that when repeated power finishing was applied, the porosity of the surface was reduced, a reduction that was shown over a pore range larger than 100 nm in their study.

In 2008, Garcia et al. [24] analyzed the use of three different DSH: quartz + corundum + cement, iron fillings + quartz + cement, and quartz + cement. In the three cases, two different application methods were used: hand finished, and power finished. Compressive strength, density, water absorption, permeability, abrasion resistance, impact resistance and chemical resistance were evaluated, concluding that, if polished, the concrete quality improved, and the quartz + cement DSH was the admixture that offered the best general-purpose quality.

Mardani-Aghabaglou et al. [17] studied the behavior of corundum aggregate and cement as a DSH. They observed that the application of DSH improved the compressive strength, elastic modulus, abrasion resistance, and drying shrinkage of the concrete. No influence of the surface coating was visible in either the test results for water absorption, depth of water penetration under pressure, or the freeze-thaw test results.

The good abrasion resistance [28], and the toughness of the EAFS shown in the literature [28], and the improved Interfacial Transition Zone (ITZ) between cementitious matrix and EAFS aggregates, in comparison with cement matrix and natural aggregates, make EAFS a good candidate to replace quartz (and other similar aggregates) for the surface treatment of concrete paving slabs, decreasing the consumption of natural raw materials, promoting environmental conservation through the recovery of EAF slag as a valuable material, and working toward the achievement of sustainable development.

In the present paper, the behavior of a surface paving coating manufactured with EAF slag and cement is evaluated and compared with the behavior of a surface coating manufactured with quartz and cement. With that purpose in mind, three EAF slag concrete slabs were built, one reinforced with metallic fibers, another with synthetic fibers, and a third with no fibers tough reinforced with bars; these typologies of paving slabs (fiber reinforced or classically reinforced) are accepted in the current engineering practice for the present application. In all three cases, one half of the surface was coating with an EAF slag mixture and the other half with quartz-based mixture, to compare both surface treatments. The slabs were left to age for 4 years outdoors, after which they were visually inspected, and tested to evaluate the surface quality in terms of impact, skid, abrasion, water absorption and oil-stain resistance.

2. Materials and methods

2.1. Specimens design

Three different concrete slabs were manufactured with three different concrete types: slag concrete with ordinary bars reinforcement (E); EAF slag concrete reinforced with metallic fibers (M); and EAF slag concrete reinforced with synthetic fibers (S). The slabs measured 2.5 × 2.5 × 0.15 m and weighed around 2600 kg.

The dosage used for concretes was described in previous articles of authors [29,30]; Table 1 displays the main parameters compositional, physical and mechanical of mixes.

Table 1
Mix proportions of concrete and additional data.

Mix design (kg/m^3)		E	EM	ES
Cement		360	360	360
Water		200	200	200
Siliceous fine aggregate (0/4 mm)		500	500	500
EAFS aggregates	Size 0/4 mm	515	515	515
	Size 4/10 mm	670	670	670
	Size 10/20 mm	550	550	550
Plasticizer (1.5 % wt. of cement)		5.4	5.4	5.4
Metallic/Synthetic Fibers		–	45	3.5
Abrams cone slump (mm)		140	130	60
Fresh density (Mg/m^3)		2.86	2.87	2.85
Compressive strength (MPa)	28 days	58.8	68.9	57.7
	90 days	72.1	80.6	62.5
Dry density (Mg/m^3)		2.46	2.53	2.45

Each slab type was coated with two dry-shake surface hardener (DSH) admixtures. Half of each slab was finished with a mix of Portland cement type I as specified in EN 197-1 [31] and quartz, in proportions of 1:2 (one part of cement and two part of aggregate). The other half of each slab was also finished with Portland cement type I and, in this case, with EAF slag in the same proportions of 1:2. The granulometries of the EAF slag and the quartz were chosen as very similar, as shown in Fig. 1.

Both coatings used amounts close to 6 kg (about 2.5 L) of dry powder sprinkled per square meter as a recommendable and usual proportion; the foreseeable thicknesses of the surface coating averaged 2.5 mm and, inevitably in practice, varied between 1.5 and 5 mm depending on the superficial regularity of substrate concrete. It was polished with mechanical scrubbing to obtain a semi-fine or anti-slip surface, suitable for use on severely run industrial pavements.

Once the base concrete course 150 mm thick had been compacted, vibrated with a ruler and smoothed with a straightedge, it started to exude water. At that point, each coating mix (EAF-cement, quartz-cement) was sprinkled on half of the slab; in Fig. 2 (left), the slab may be seen after the addition of the dry-shake hardener. It was then necessary to wait for the concrete to gain the right consistency before using the concrete helicopter for mechanical scrubbing, as shown in Fig. 2 (Right).

In Table 2, the identification and configuration of the slab is presented: concrete type and surface treatment type and the manufactured slabs are shown in Fig. 3, divided into concrete types and surface treatment type. Summarizing, odd numbers (1,3,5) are slab surfaces with cement/quartz coatings and even numbers (2,4,6) are slab surfaces with cement/EAF slag coatings.

2.2. Test methods

Before evaluating the behavior of the different mixes used in the surface coating of the slabs, they were placed outdoors for aging over 4 years at the city of Burgos (northern Spain), at an altitude of 856 m above sea level. The climate in Burgos is quite extreme (temperate continental): cold in winter and hot in summer. In addition, temperatures below 10 °C at nighttime and over 30 °C in the daytime have been recorded in summertime, on the same day.

After the four-year ageing period, the slabs were visually inspected, looking for possible imperfections or macro-defects, as flaws, cracking, chipping, and spots … and paying special attention to the differences among the surface coatings. Then, the skid and the oil stain resistances of the slab surface coatings were measured. Cylindrical samples with diameters of 150 mm were taken from the slabs to perform impact, abrasion, and short- and long-term water-absorption tests.

The skid resistance of the surface was measured with the Transport Road Research Laboratory (TRRL) pendulum, as specified in EN 13036-4 “Road and airfield surface characteristics - Test methods - Part 4: Method for measurement of skid resistance of a surface: The pendulum test” [31]. The pendulum has a standardized rubber coated slider, which slides along the surface of the slab. The arm of the pendulum is initially placed horizontally and, when it descends, the friction decelerates the arm, and the needle will mark the residual swing on a scale (show Fig. 4). The results are expressed on a scale based on a “Pendulum Test Value” (PTV); the greater the friction (less slipperiness), the higher the PTV value.

The impact test was performed as per UNE 83514 [32] (taking into account that some of the concrete mixes contained fibers). The drilled samples were taken with a 63 mm high and 150 mm diameter, hollow water-cooled drill, as specified in the standard. The test device consisted of a metallic tenderizer with a circular base of 4.54 kg attached to a tubular guide, as shown in Fig. 5. The specimens were placed on the base sheet, centered between four platens. A metallic ball was placed above the specimen and at the center. In the test, the tenderizer falls from a height of 427 mm onto the ball and the indentation caused by the impact is measured using an analogue micrometer, connected to a tripod, yielding the difference between the specimen surface and the indentation mark. Measurements were taken every two falls of the tenderizer.

The abrasion test was performed following the specifications described in UNE-EN-1338 [31]. As in the previous test, transversal specimens measuring 150 mm in diameter and 63 mm in height were used.

With the aim of simulating pavement behavior under rainy and snowy conditions, two different tests were designed to evaluate short- and long-term pavement water absorption. These tests were also carried out to evaluate the porosity of the mixes; porosity is closely linked to the aggregate-matrix interface, strength and deformability of the concretes [33], so evaluating one property makes it possible to have an idea of the others. Both tests were performed on the same transversally drilled samples.

Designed to evaluate short-term water absorption, the test involved sealing a funnel-shaped glass separation column (show Fig. 6)

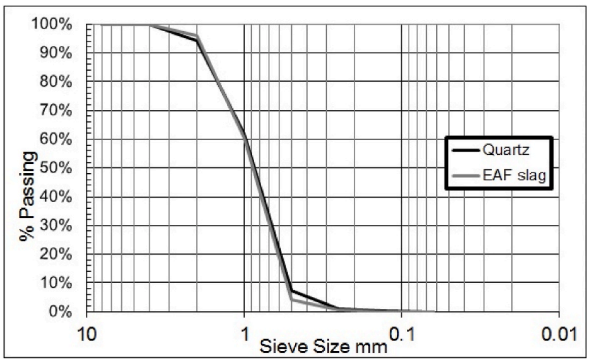

Fig. 1. Granulometry curve of the coating course aggregates.

Fig. 2. Mix extended in the slab (Left); Mechanical scrubbing with concrete helicopter (Right).

Table 2
Slab and coating types.

Concrete + Reinforced Steel **(E)** Cement-Quartz Surface Coating **(EC)**	**1**	**E**	**2**	Concrete + Reinforced Steel **(E)** Cement-EAF Slag Surface Coating **(EE)**
Concrete + Steel Fibers (**M**) Cement-Quartz Surface Coating (**MC**)	**3**	**M**	**4**	Concrete + Steel Fibers (**M**) Cement-EAF Slag Surface Coating (**ME**)
Concrete + Synthetic Fibers (**S**) Cement-Quartz Surface Coating (**SC**)	**5**	**S**	**6**	Concrete + Synthetic Fibers (**S**) Cement/EAF Slag Surface Coating (**SE**)

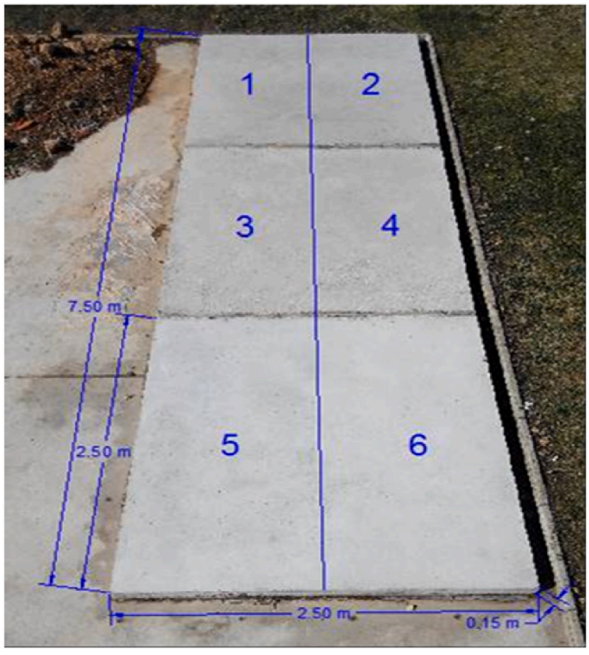

Fig. 3. Slab dimensions and labels.

with a diameter of 25 mm attached to the surface of the sample with plasticine. The column was filled with water up to the last graduation line (total volume 4 ml). The water was introduced through a burette, so that the filling rate was the same for all the samples. Once the column was full, the time it took for the water to drop 4 ml was measured or the sample was left for 30 min within which time the column was emptied. The results reflect the water absorption coefficient of the treatment surface, calculated as the volume of water absorbed, divided by the surface (circle of 25 mm) and the time (emptying time for 4 ml or 30 min).

The test developed to measure the long-term water absorption of the surfaces (really a test of capillary permeation) consisted in placing a 70–80 mm high plastic collar around the sample and sealing it with silicon. The core sample was then weighed, and the vessel/receptacle formed by the sample and the collar was filled with water (0.75 l) (show Fig. 7). It was then left for 72 h, in accordance with the RILEM recommendations for water absorption by capillarity of concrete (RILEM CPC 11.2) [34]. When the time

Fig. 4. British Pendulum Number (BPN) portable skid-resistance tester.

Fig. 5. Impact testing device.

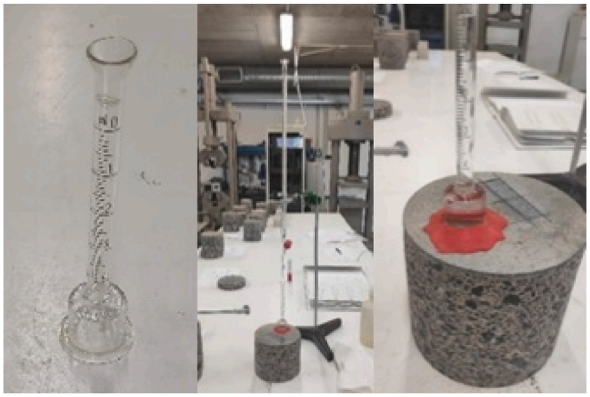

Fig. 6. Short-term water absorption test.

had elapsed, the vessel must be emptied and dried and the sample was then weighed again. The results are presented as estimates of the absorbed/permeated water using the difference in sample weight before and after the test and calculating the absorption rate coefficient, taking into account the time (72 h) and the test surface (in this case, a 130 mm diameter circle).

Finally, oil stain resistance was measured, in order to establish the resistance of the surface finish to oil stains from engine leaks, a capital question in industrial and road pavements. The test took place *in situ* on the slabs. It consisted of pouring 50 ml of motor oil on each half-slab and spreading it with a sponge. It was then left for different periods of time: 15 min, 1 h, and 24 h. After each period, it was cleaned with hot water for 1 min with a pressurized water washing machine and its appearance was observed, after which the results were recorded.

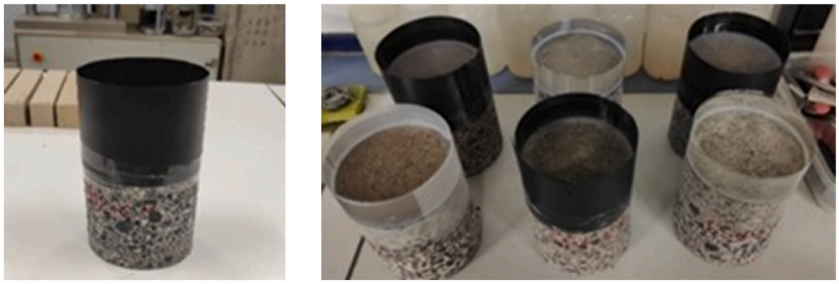

Fig. 7. Long-term water absorption test.

3. Results and discussion

3.1. Visual inspection

After 4 years of exposure to weathering, the condition of the surface coating of the slab was generally good, though not perfect. No color differences between the two slab coatings were observed.

Small surface cracks [35] could be appreciated on the edges of the first slab manufactured with slag concrete without fiber (E, Fig. 8) that only affected the surface coating [36]. The cracks appeared in the initial moments, due to a quicker speed of water evaporation that was insufficiently compensated by the exuded water [37,38] and the scarcity of exudation near the contours. The proportion of cracks found in both coatings was similar as shown in Fig. 8 (EC, EE, left). These cracks had a negligible influence on concrete durability, because their depths were estimated in around 1 mm, introducing a vertical thin metallic sheet, and do not reach the base material; the only negative aspect of that cracking was aesthetic.

The appearance of the second slab, M, manufactured with slag concrete reinforced with metallic fibers was better than the previous one. Only few extensions having cracks may be observed on the contour of slabs, see Fig. 8 (right), evidencing a more abundant exudation associated to more proportion of mixing water. No significant differences between the cracks on the two coatings were visible. Also, some oxidized metallic fibers were noted, due to the contact of the fiber with the ambient moisture. Those fibers were randomly visible, similar in the part of the slab finished with slag and with quartz.

On the third slab S, manufactured with slag concrete and reinforced with synthetic fibers, the small cracks seen on the other slabs were not visible. In this case, a different behavior was seen between both type of coatings; on the half of the slab coated with quartz, small chips between 15 mm and 30 mm began to appear, as shown in Fig. 9. However very little chipping was evident in the half-slab coated with EAF slag.

In Fig. 10, the chips are shown either in red or in yellow, on the halves coated with quartz and with EAF slag, respectively. In this way, it is possible to appreciate the quantity and the location of the chips and, in general, they coincided with the presence of a synthetic fiber. Assuming that the presence of emerging synthetic fibers is randomly distributed in the surface of the basis concrete, it is difficult to state a convincing reason justifying this behavior; apparently, the presence of slag is a favorable factor to hide the emergent fibers. In general, a better behavior of one coating rather than another cannot be affirmed based on the visual inspection, with the exception of the synthetic fiber slabs. A key question is the rate of superficial water exudation from the basic concrete of slabs, which is a question more related with basis concrete properties than with the coating mortars. Undoubtedly, the unavoidable presence of reinforcing fibers in the surface of M and S slabs is decisive in their aesthetic appearance, being iron oxidation points or being chips in plastic fibers.

3.2. Skid resistance

The skid resistance of the surface coatings was measured on the three different slabs and on both DSH types, as described above.

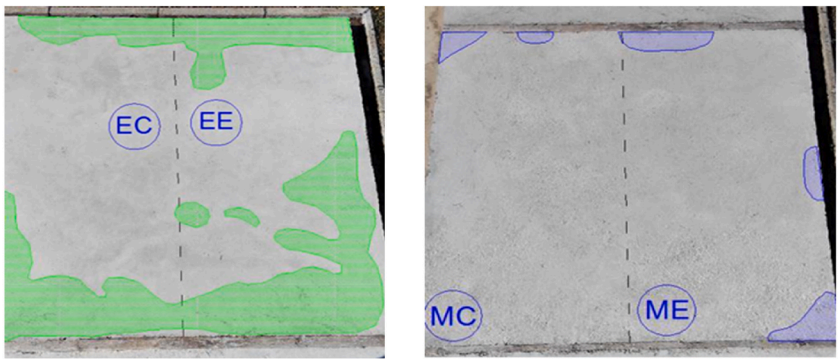

Fig. 8. Distribution of surface cracking in E (left) and EM slabs (right).

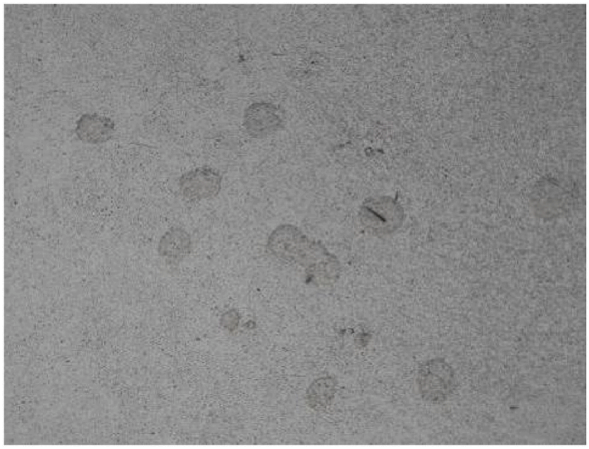

Fig. 9. Chips found in the slab upper face.

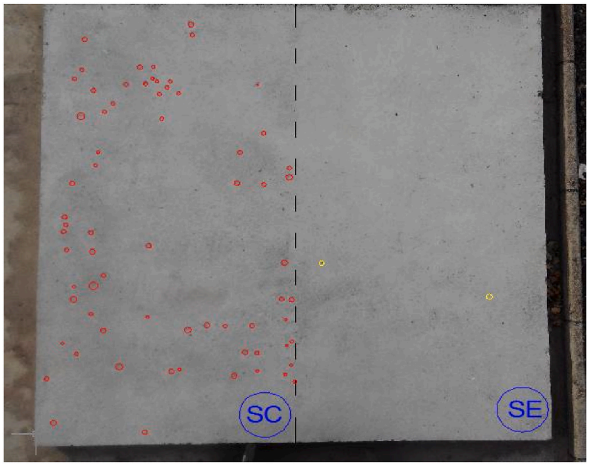

Fig. 10. Location of chipping on the slag concrete slab with synthetic fibers.

The test was developed on dry and wet surfaces, 3 measurements on each half-slab were taken per slab type in regions/zones free of superficial defects. In Table 3, the averages of the 3 measurements on each half-slab when dry and when wet are shown.

As was predictable, the wet pavement results were slightly worse than the dry pavement results. In general, the data for both pavements, even when wet, were good. Four different values for floor types are defined in the CTE-DB-SUA 1, the Spanish technical building code [39] on safety measures against the risk of falls, depending on skid resistance measured on a wet floor, as shown in Table 4.

In this case, both the quartz and the slag top coatings can be classified as class 3, the class with the best behavior of the four classes presented in the code.

Furthermore, considering the suggested minimum British Pendulum Numbers (BPN) measured with the portable tester according to TRRL recommendations for roads [40], shown in Table 5, all values can be considered as Category A, except for the EE slab with a slag top coating, which was Category B. Hence, the skid resistance of the concrete slab coated with EAF slag as a DSH admixture was sufficient for almost all uses.

The skid resistance has classically two components: adhesion and hysteresis and depends on both surface macro and micro-textures. Macrotextures are considered as vertical and horizontal surface irregularities between 0.1 mm and 20 mm and between 0.5 and 50 mm, respectively, and micro-textures are surface irregularities between 10^{-3} and 0.5 mm vertically and less than 0.5 mm horizontally [41]. Concerning the macro textures, the concrete of the underlying course was shown to influence this skid resistance. The pavement manufactured with no fibers had less skid resistance than the pavements manufactured with fibers, which has reflected the suitable macrotexture of the final surface due to the fiber concrete of basis.

The micro-texture is theoretically influenced by water cement ratio, aggregate content, fineness modulus, and surface roughness/mineralogy of the fine particles [42]. In this case, the difference in the micro-texture of both coating types is due to the different surface roughness and particle mineralogy of the used aggregates, all other variables remaining constant. The quartz is a material harder (7 units in the Mosh scale) and more abrasive than the EAF slag, whose content in olivine and iron oxides mitigate these properties,

Table 3
Skid resistance results.

Specimens	Dry Slab	Wet Slab
EE	66	63
ME	75	69
SE	74	70
EAF slag	**72**	**67**
EC	71	68
MC	80	72
SC	77	73
Quartz	**76**	**71**

Table 4
Floor slipperiness classifications [39].

Skid Resistance [PTV]	Class
$Rd \leq 15$	0
$15 < Rd \leq 35$	1
$35 < Rd \leq 45$	2
$Rd \geq 45$	3

Table 5
Minimum BPN for different sites according to the Transport Road Research Laboratory (TRRL) [40].

Category	Type of site	Minimum skid resistance (wet surfaces)
A	Difficult sites such as: 1. Roundabouts 2. Bends with a radius of less than 150 m on unrestricted roads 3. Gradients 1 in 20 or steeper of lengths greater than 100 m 4. Approaches to traffic lights on unrestricted roads	65
B	Motorways, trunk and class 1 roads and roads with heavy traffic in urban areas (over 2000 vehicles per day)	55
C	All other sites	45

leading to hardness close to felspars (6 units in the Mosh scale). In the upper face of these coated pavements, and due to the final scrubbing, we find the "greater" fine aggregate particles (sized above 0.2 mm) solidly hold by a high-quality cementitious matrix; their influence in the skip resistance against rubber/elastomers is capital.

3.3. Impact resistance

In Table 6, the results of the Impact test, divided by the type of concrete and the top coating, are shown. The hollow depth of each two blows is measured in millimeters, and it can be observed that the set of deep results do not exceed the thickness of the finishing course (around 2.5 mm); obviously its influence is predominant.

Additionally, In Fig. 11, the relation between number of blows and the indentation depth is shown for the two top coatings. Up until Blow 4, the two surface coatings showed similar behaviors. From that point, the slag surface coating was smaller, i.e. more favorable) than the quartz top coating, with a difference of 0.51 mm between the indentation depths on Blow 16, 54 % higher in the case of quartz. Impact resistance is related with the capability of the materials to absorb/dissipate the impact energy. These results agree to those of

Table 6
Average indentation depth per two blows.

Specimens	Indentation depth (mm) for each number of blows							
	2	4	6	8	10	12	14	16
EE	0.27	0.35	0.44	0.48	0.53	0.57	0.66	0.79
ME	0.20	0.27	0.34	0.38	0.60	0.73	0.83	0.89
SE	0.29	0.42	0.54	0.59	0.74	0.94	0.99	1.10
EAF slag	**0.25**	**0.35**	**0.44**	**0.48**	**0.62**	**0.75**	**0.83**	**0.93**
EC	0.36	0.44	0.64	0.86	1.21	1.25	–	–
MC	0.18	0.30	0.35	0.39	0.50	0.70	1.10	1.52
SC	0.16	0.37	0.48	0.66	0.78	0.91	1.13	1.36
Quartz	**0.23**	**0.37**	**0.49**	**0.64**	**0.83**	**0.95**	**1.12**	**1.44**

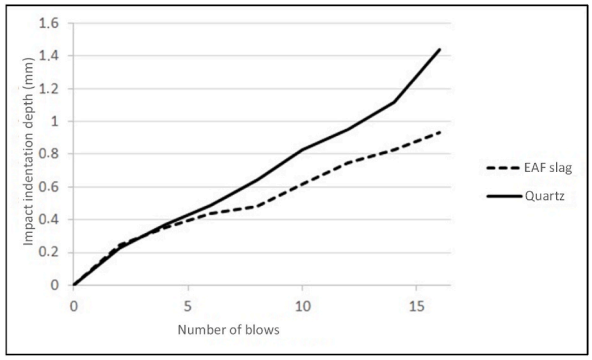

Fig. 11. Impact resistance of quartz and EAF slag top coatings.

Garcia et al. [24], quartz is a brittle material with low energy-absorption levels; however, electric arc furnace slag is a more compliant and tougher material, so its capability to absorb/dissipate impact energy is advantageous with respect the quartz.

3.4. Abrasion resistance

The abrasion resistance test was developed on the surface coating of the transversally drilled cylinder, as shown in Fig. 12. The results of the test in Table 7 showed that in this case both the basic pavement concrete type and the surface (finishing) coating influenced slab abrasion resistance as it has been seen in by other authors [25]. The difference between the results of the different surface coatings was small, although the behavior of the quartz surface coating was slightly better, in coherence with the higher resistance to abrasion of quartz.

All obtained results can be considered acceptable values, in so far as the most restrictive abrasion values in the EN1338 standard [31] are less than 20 mm, which correspond to a CE type I marking. In this study, both values were below that limit. The following abrasion resistance limits are also specified in UNE 127748 [32]: pavements for normal usage should be less than 25 mm; pavements for intensive usage, less than 23 mm; and pavements for industrial usage, less than 21 mm. So, the EAF slag surface coating results could even be appropriate for industrial pavements.

3.5. Water absorption

The short-term water-absorption test results were that neither the quartz nor the EAF slag surface coatings absorbed water; the volume of absorbed water in both cases was null after 30 min, as evidence of the suitable quality of coating courses.

The data on long-term water absorption by capillarity are shown in Table 8, as a measure of the global (coating and basis) permeability. Absorption levels were low, and all absorption coefficients were smaller than 50 $g/m^2 \cdot min^{0.5}$, a good value in hydraulic mixes (remember the less permeable mortars, which must show a value of 200 $g/m^2 \cdot min^{0.5}$). In general, the absorption of the EAF slag coating was higher than the quartz top coating, being the reason justifying the higher water absorption/permeability of the EAF slag aggregates compared with the quartz. The influence of the basic concrete is also revealed in the results of Table 8, not only due to their own properties, but due to the quality of their top course, which is constituted as a barrier against the penetration of liquid substances. The synthetic fibers concrete in basis leads to the more permeable coating, in a similar way to that showed in the former section 3.1 of visual inspection, in which the chips presence in SE/SC was the most notable indication.

3.6. Oil stain resistance

In Table 9, the qualitative results for each half-slab after oil-stain cleaning are shown. It can be seen that the surface coating had no influence on the cleaning process; instead, the type of basic slab concrete had the most influence. The concrete without fibers obtained

Fig. 12. Specimen testing and traces marked on the top coatings of the test specimens.

Table 7
Abrasion test results.

Specimens	Abrasion resistance (mm)
EE	15.5
ME	17.5
SE	18.5
EAF slag	**17.2**
EC	15.0
MC	17.0
SC	18.0
Quartz	**16.7**

Table 8
Water absorption test results.

Specimens	Water absorption [% in weight]	Water absorption coefficient [$g/m^2 \cdot min^{0.5}$]
EE	0.53	30.8
ME	0.63	37.5
SE	0.85	49.1
EAF slag	**0.64**	**39.1**
EC	0.25	14.5
MC	0.37	22
SC	0.75	43.3
Quartz	**0.46**	**26.6**

Table 9
Oil stain resistance test results.

Specimens	Appearance after 15 min	Appearance after 1 h	Appearance after 24 h
EC	Totally removed	Still slightly stained	Still slightly stained
EE	Totally removed	Still slightly stained	Still slightly stained
MC	Totally removed	Still slightly stained	Visibly stained
ME	Totally removed	Still slightly stained	Visibly stained
SC	Still slightly stained	Still slightly stained	Visibly stained
SE	Still slightly stained	Still slightly stained	Visibly stained

the best cleaning results, undoubtedly due to it being the most impermeable ensemble basis/coating, as the results of the water absorption test showed and has been demonstrated elsewhere [29,30]. On the other hand, the slab with synthetic fibers had the worst results for cleaning and showed the highest permeability in the aforementioned tests.

4. Conclusions

In this study, a new application for EAF slag in a hydraulic cement matrix forming a thin course on pavements (DSH, dry shake hardener) has been investigated. Based on the experimental results, the following conclusions can be drawn:

- From a visual inspection, it can be concluded that the behavior of the quartz surface coating and the EAF slag surface coating were very similar. In any case, the EAF slag coating had a slightly better behavior, being more compatible with the synthetic fibers.
- Quartz surface coatings showed slightly better skid resistance than slag surface coatings. Nevertheless, the difference between them was small and both surface coatings could be considered as acceptable under the engineering point of view.
- The impact resistance of the EAF slag surface coating was better than the quartz top coating. Furthermore, the resistance to abrasion of both top coatings was similar, with almost negligible differences.
- The short-term water absorption of both surface coatings was null, and was small in the long term, revealing an excellent performance of both coating types. The water permeability levels of the ensemble slag surface coating - basic slag concrete, were higher than those of quartz surface coating.
- No difference was observed in the oil stain resistance of both surface coatings, in this case the different behaviors were linked to the base concrete and not the surface coating.

Based on these conclusions, the EAF slag is "*a priori*" a suitable material for use in the surface treatment of concrete slabs for indoor use and for outdoor use under severe climatic conditions. Nevertheless, further analyses will have to be developed before EAF slag may be included as a DSH in engineering standards.

CRediT authorship contribution statement

Amaia Santamaría: Writing – original draft, Writing – review & editing. **Vanesa Ortega-López:** Conceptualization, Investigation, Methodology. **Marta Skaf:** Investigation, Methodology. **Victor Revilla-Cuesta:** Investigation, Methodology. **J.M. Manso:** Funding acquisition, Project administration, Supervision.

Declaration of competing interest

The authors declare that they have no known competing financial interests or personal relationships that could have appeared to influence the work reported in this paper.

Data availability

No data was used for the research described in the article.

Acknowledgments

The authors wish to express their gratitude to the following funding entities MCIN/AEI/10.13039/501100011033, "ERDF A way of making Europe"; the "European Union", NextGeneration EU/PRTR [PID2020-113837RB-I00; PID2021-124203OB-I00 and TED2021-129715B–I00]; the Junta de Castilla y León (Regional Government) and ERDF [UIC-231, BU11917]; the Basque Government [IT1619-22 SAREN research group]; and Burgos University [Y135.GI].

References

[1] S.A. Ihobe, Libro blanco para la minimización de residuos y emisiones, escorias de acería., 1999.
[2] M. Pasetto, G. Giacomello, E. Pasquini, F. Canestrari, Effect of warm mix chemical additives on the binder-aggregate bond strength and high-service temperature performance of asphalt mixes containing electric arc furnace steel slag, RILEM book Series 11 (2016) 485–496.
[3] J.M. Manso, D. Hernández, M.M. Losáñez, J.J. González, Design and elaboration of concrete mixtures using steelmaking slags, ACI Mater. J. 108 (2011) 673–681.
[4] S.I. Abu-Eishah, A.S. El-Dieb, M.S. Bedir, Performance of concrete mixtures made with electric arc furnace (EAF) steel slag aggregate produced in the Arabian Gulf region, Construct. Build. Mater. 34 (2012) 249–256.
[5] F. Faleschini, P. De Marzi, C. Pellegrino, Recycled concrete containing EAF slag: environmental assessment through LCA, Eur J Environ Civ Eng 18 (2014) 1009–1024.
[6] V. Ortega-López, A. García-Llona, V. Revilla-Cuesta, A. Santamaría, J.T. San-José, Fiber-reinforcement and its effects on the mechanical properties of high-workability concretes manufactured with slag as aggregate and binder, J. Build. Eng. 43 (2021), 102548.
[7] M. Skaf, J.M. Manso, Á. Aragón, J.A. Fuente-Alonso, V. Ortega-López, EAF slag in asphalt mixes: a brief review of its possible re-use, Resour. Conserv. Recycl. 120 (2017) 176–185.
[8] M. Pasetto, E. Pasquini, G. Giacomello, A. Baliello, Life-Cycle Assessment of Road Pavements Containing Marginal Materials: Comparative Analysis Based on a Real Case Study, Pavement Life-Cycle Assessment, 2017, pp. 199–208.
[9] G. Adegoloye, A. Beaucour, S. Ortola, A. Noumowé, Concretes made of EAF slag and AOD slag aggregates from stainless steel process: mechanical properties and durability, Construct. Build. Mater. 76 (2015) 313–321.
[10] N. Rojas, M. Bustamante, P. Muñoz, K. Godoy, V. Letelier, Study of properties and behavior of concrete containing EAF slag as coarse aggregate, Dev. Built Environ. 14 (2023), 100137.
[11] F. Faleschini, L. Hofer, M.A. Zanini, M. dalla Benetta, C. Pellegrino, Experimental behavior of beam-column joints made with EAF concrete under cyclic loading, Eng. Struct. 139 (2017) 81–95.
[12] B. Fronek, P. Bosela, N. Delatte, Steel slag aggregate used in Portland cement concrete: US and international perspectives, Transport. Res. Rec.: J. Transport. Res. Board 2267 (2012) 37–42.
[13] N.H. Roslan, M. Ismail, N.H.A. Khalid, B. Muhammad, Properties of concrete containing electric arc furnace steel slag and steel sludge, J. Build. Eng. 28 (2020), 101060.
[14] I. Arribas, J.T. San-José, I.J. Vegas, J.A. Hurtado, J.A. Chica, Application of steel slag concrete in the foundation slab and basement wall of the Labein-Tecnalia Kubik building. 6th European Slag Conference, EUROSLAG pub, 2010.
[15] J.L. García Mochales, Utilización de áridos siderúrgicos en obras por la autoridad portuaria de Bilbao, 2016.
[16] P.C. Taylor, G.F. Voigt, Integrated Materials and Construction Practices for Concrete Pavement: A State-Of-The-Practice Manual, United States. Federal Highway Administration. Office of Pavement Technology, 2007.
[17] A. Mardani-Aghabaglou, K. Karakuzu, V. Kobya, D. Hatungimana, Durability performance and dimensional stability of road concrete containing dry-shake surface hardener admixture, Construct. Build. Mater. 274 (2021), 121789.
[18] Q. Dong, X. Cao, S. Wang, X. Chen, B. Yang, S. Xie, et al., Design and evaluation of an innovative composite silicate-based surface treatment agent of concrete, Case Stud. Constr. Mater. 18 (2023), e02207.
[19] X. Pan, Z. Shi, C. Shi, T. Ling, N. Li, A review on surface treatment for concrete – Part 2: performance, Construct. Build. Mater. 133 (2017) 81–90.
[20] X. Pan, Z. Shi, C. Shi, T. Ling, N. Li, A review on concrete surface treatment Part I: types and mechanisms, Construct. Build. Mater. 132 (2017) 578–590.
[21] J. He, C. Qiao, Y. Farnam, Durability evaluation of reinforced concrete with surface treatment of soy methyl ester-polystyrene under freeze-thaw cycles and calcium chloride, Cement Concr. Compos. 137 (2023), 104927.
[22] F. Wu, X. Chen, J. Chen, Abrasion resistance enhancement of concrete using surface treatment methods, Tribol. Int. 179 (2023), 108180.
[23] M. Collepardi, E.N. Croce, G. Fazio, Olagot Jjo, R. Troli, ASR-Free Dry Shake Hardeners for Concrete Industrial Floors, SP-234, American Concrete Institute, ACI Special Publication, 2006, pp. 747–754.
[24] A. García, D.C. Fresno, J.A. Polanco, Effect of dry-shaking treatment on concrete pavement properties, Construct. Build. Mater. 22 (2008) 2202–2211.
[25] A. García, D. Castro-Fresno, J.A. Polanco, C. Thomas, Abrasive wear evolution in concrete pavements, Road Mater. Pavement Des. 13 (2012) 534–548.
[26] A. García Hernández, Desarrollo y análisis de Pavimentos Industriales desde el punto de vista de acabado superficial, Tesis doctoral, 2007.
[27] M. Sadegzadeh, C.L. Page, R.J. Kettle, Surface microstructure and abrasion resistance of concrete, Cement Concr. Res. 17 (1987) 581–590.
[28] I. Arribas, A. Santamaría, E. Ruiz, V. Ortega-López, J.M. Manso, Electric arc furnace slag and its use in hydraulic concrete, Construct. Build. Mater. 90 (2015) 68–79.
[29] J. Fuente-Alonso, V. Ortega-López, M. Skaf, Á. Aragón, J.T. San-José, Performance of fiber-reinforced EAF slag concrete for use in pavements, Construct. Build. Mater. 149 (2017) 629–638.

[30] V. Ortega-López, J.A. Fuente-Alonso, A. Santamaría, J.T. San-José, Á. Aragón, Durability studies on fiber-reinforced EAF slag concrete for pavements, Construct. Build. Mater. 163 (2018) 471–481.
[31] CEN European Commitee for Standarization. Rue de Stassart, vol. 36. Brussels B-1050.
[32] AENOR. UNE Standards.
[33] J.T. San-José, I. Vegas, A. Ferreira, Reinforced polymer concrete: physical properties of the matrix and static/dynamic bond behaviour, Cement Concr. Compos. 27 (2005) 934–944.
[34] Rilem Tc, CPC 11.2 Absoption of water by concrete by capillarity, in: RILEM (Ed.), RILEM Recommendations for the Testing and Use of Construction Materials; 1994, 1982, pp. 34–35.
[35] K. Chaiyasarn, A. Buatik, H. Mohamad, M. Zhou, S. Kongsilp, N. Poovarodom, Integrated pixel-level CNN-FCN crack detection via photogrammetric 3D texture mapping of concrete structures, Autom. ConStruct. 140 (2022), 104388.
[36] G. Tiberti, A. Mudadu, B. Barragan, G. Plizzari, Shrinkage cracking of concrete slabs-on-grade: a numerical parametric study, Fibers 6 (2018).
[37] J. Liu, N. Farzadnia, C. Shi, X. Ma, Shrinkage and strength development of UHSC incorporating a hybrid system of SAP and SRA, Cement Concr. Compos. 97 (2019) 175–189.
[38] V. Revilla-Cuesta, L. Evangelista, J. de Brito, M. Skaf, J.M. Manso, Shrinkage prediction of recycled aggregate structural concrete with alternative binders through partial correction coefficients, Cement Concr. Compos. 129 (2022), 104506.
[39] Ministerio Español de Transportes, Movilidad y Agenda Urbana, Documento Básico SUA. SUA1 Seguridad frente a riesgo de caídas, in: Anonymous Códito Técnico de la Edificación, 2022.
[40] TRRL, Instructions for using the portable skid tester, in: Anonymous Transport and Road Research Laboratory HMSO, 1969, p. 27. Road Note.
[41] F.G. Praticò, A. Astolfi, A new and simplified approach to assess the pavement surface micro- and macrotexture, Construct. Build. Mater. 148 (2017) 476–483.
[42] W. Zhao, J. Zhang, J. Lai, X. Shi, Z. Xu, Skid resistance of cement concrete pavement in highway tunnel: a review, Construct. Build. Mater. 406 (2023), 133235.